

Organic & Biomolecular Chemistry

Accepted Manuscript



This article can be cited before page numbers have been issued, to do this please use: J. F. Miravet, B. Escuder and C. Berdugo, *Org. Biomol. Chem.*, 2014, DOI: 10.1039/C4OB02003K.



This is an *Accepted Manuscript*, which has been through the Royal Society of Chemistry peer review process and has been accepted for publication.

Accepted Manuscripts are published online shortly after acceptance, before technical editing, formatting and proof reading. Using this free service, authors can make their results available to the community, in citable form, before we publish the edited article. We will replace this *Accepted Manuscript* with the edited and formatted *Advance Article* as soon as it is available.

You can find more information about *Accepted Manuscripts* in the [Information for Authors](#).

Please note that technical editing may introduce minor changes to the text and/or graphics, which may alter content. The journal's standard [Terms & Conditions](#) and the [Ethical guidelines](#) still apply. In no event shall the Royal Society of Chemistry be held responsible for any errors or omissions in this *Accepted Manuscript* or any consequences arising from the use of any information it contains.

ARTICLE

Structural Insight into the Aggregation of L-Prolyl Dipeptides and its Effect on Organocatalytic Performance

Cite this: DOI: 10.1039/x0xx00000x

Cristina Berdugo,^a BeatriuEscuder,^{a*} and Juan F. Miravet^{a*}Received 00th January 2012,
Accepted 00th January 2012

DOI: 10.1039/x0xx00000x

www.rsc.org/

NMR and organocatalytic studies of four dipeptides derived from L-proline are described. Results indicate that important conformational changes around the catalytic L-proline moiety are observed for free dipeptides upon changing the adjacent amino acid. Also, an aggregation process is detected as the concentration increases. Self-association of the dipeptides has been fitted to a cooperative binding model. All the compounds have been assayed as catalysts for the conjugated addition of cyclohexanone to *trans*- β -nitrostyrene in toluene. In agreement with the structural studies, noticeable changes in the catalytic performance are detected upon changing catalyst concentration, being the catalyst activated by self-aggregation.

Introduction

Organocatalysis has become a major topic of research in organic chemistry during the last decades. The extensive work in this area has been reviewed very often and examples can be found of organocatalysts for quite a variety of reactions and media.¹ An outstanding family of organocatalysts is that derived from peptides and in particular from L-proline. This kind of catalysts have been reported successfully in asymmetric catalysis for a wide range of synthetically reactions.² Focusing on the reaction studied in the present work, L-proline derivatives have been used extensively as catalysts for conjugate addition reactions. Seminal work by List and coworkers reported first the use of L-proline³ and then of L-prolyl-peptides⁴ to catalyse efficiently the conjugate addition of cyclohexanone to β -nitrostyrene. Wennemers and coworkers have studied in detail peptide catalysed conjugated additions to nitroalkanes with excellent efficiency in terms of conversion and enantioselectivity.⁵ Advances in this line of research comprise the achievement of highly efficient 1,4-addition of aldehydes to nitroolefins using a continuous flow system containing solid-supported peptidocatalysts.⁶ Not long ago, a detailed mechanistic study including the determination of the stereoselectivity-determining step for this type of reaction has been described.⁷

Although catalyst aggregation is sometimes neglected, there is a growing interest in addressing this behaviour and how it affects to catalytic performance. Aggregation effects have been analysed especially for thiourea catalysts⁸ and smart strategies have been developed to avoid this undesired assembled

process.⁹ Non-linear effects in organocatalysis have been in some cases correlated with catalyst self-aggregation.¹⁰ Recently, the aggregation of catalytic L-proline containing block copolymers was studied.¹¹ Previous work reported in our group shows how the aggregation of bolaamphiphilic organogelators containing L-proline catalytic moieties into fibrillar gel networks modified the enantioselectivity of the reaction when compared to solution.¹² Also in that work the dipeptide soluble catalyst **ProValPr** (see Figure 1) was preliminary studied.

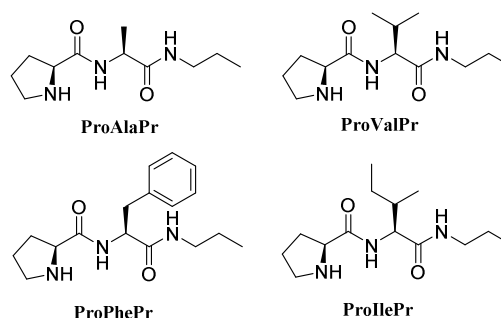


Figure 1. Structure of the catalytic dipeptides.

Here we report a detailed study of compound **ProValPr** and three other dipeptide analogues as catalysts, focusing on their structural analysis. Special attention is paid to the conformational preferences of these analogues and to their self-association in solution. Additionally, the efficiency of these molecules as catalysts in the conjugated addition of cyclohexanone to β -nitrostyrene is evaluated.¹³

The present study aims to highlight the complexity of L-prolyl catalysts associated to conformational mobility and self-aggregation rather than to develop new catalysts with high enantioselectivity, which have been reported elsewhere as cited above.

Results and Discussion

Four different L-proline derivative dipeptides were studied containing respectively L-alanine, L-phenylalanine, L-valine and L-isoleucine. All of them were capped at C-terminus as propylamides (Figure 1). The self-assembly of the dipeptide catalysts in toluene was studied from a thermodynamic and structural point of view using NMR experiments. The compounds were fully soluble in this solvent in all the concentration range studied. Firstly, self-association of the molecules was monitored by NMR in D_8 -toluene following the chemical shift of the amide signals. It can be seen in Figure 2 that both amide resonances of **ProIlePr** were shifted downfield as the concentration increases, revealing intermolecular association by means of hydrogen bonding. A similar behaviour was observed for the other compounds.

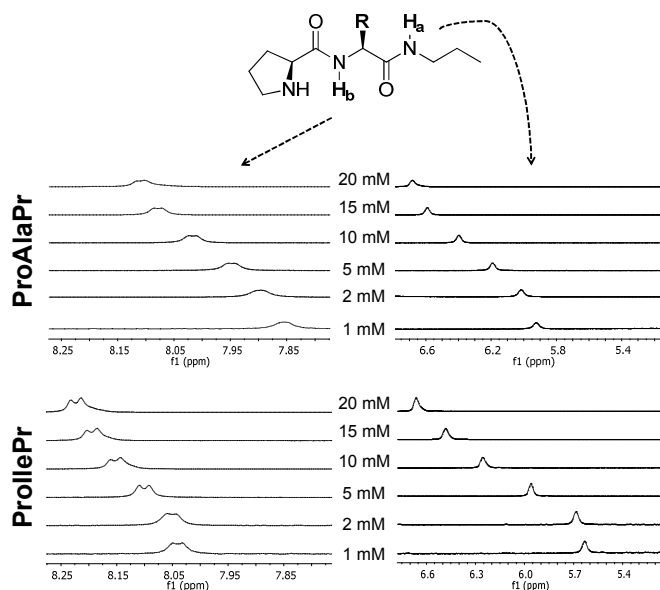


Figure 2. Partial ^1H NMR spectra of **ProIlePr** and **ProAlaPr** in D_8 -toluene at different concentrations.

Data corresponding to the shift of amide resonances upon increasing concentration could be fitted to a supramolecular polymerization model with a dimerization constant, K_2 , and equivalent successive aggregation constants, K_n (see Experimental Section and Supporting Information). In all the cases moderate cooperativity was observed being $K_n > K_2$ (Table 1). The association constants K_2 were similar for the four dipeptides but higher values of K_n were obtained for **ProValPr** and **ProIlePr**. However these differences do not affect very significantly to the proportion of aggregated species in the range of concentrations studied for catalysis. As

exemplified in Figure 3, species distribution diagram reveals that upon going from ca. 1 mM to 5 mM a very important linear increase of dimeric species takes place. Also exponential growth of oligomeric species is observed.

Molecular mechanics calculations (AMBER* force field) for the free catalysts predict in all the cases two energetically close folded conformations (ΔE ca. 7 kJ mol $^{-1}$) near the global minimum. In both cases the conformers contain a H-bond between propylamide NH and CO of the proline moiety, in accordance with the experimental results described below (see *anti* and *syn* conformers in Scheme 1; consult Supporting Information for pictures of the molecular models; details of computations in Experimental Section).

Table 1. Thermodynamic constants for the self-aggregation of the catalysts at 30 °C in toluene.

Compound	K_2	K_n	Aggregation degree at 1 mM (%) ^a	Aggregation degree at 5 mM (%) ^a
ProValPr	29	100	6	28
ProIlePr	20	106	4	24
ProPhePr	17	38	3	16
ProAlaPr	21	72	4	21

^[a] Calculated using K_2 and K_n values. Estimated error is ca. 3%.

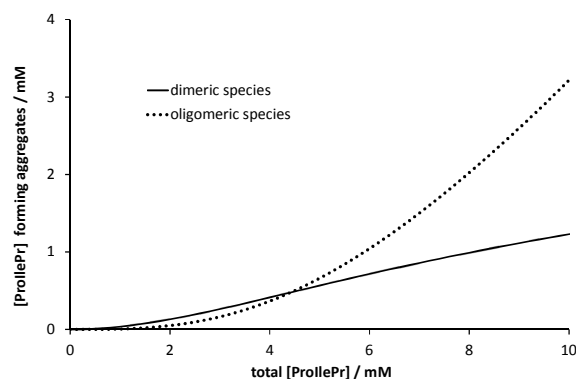
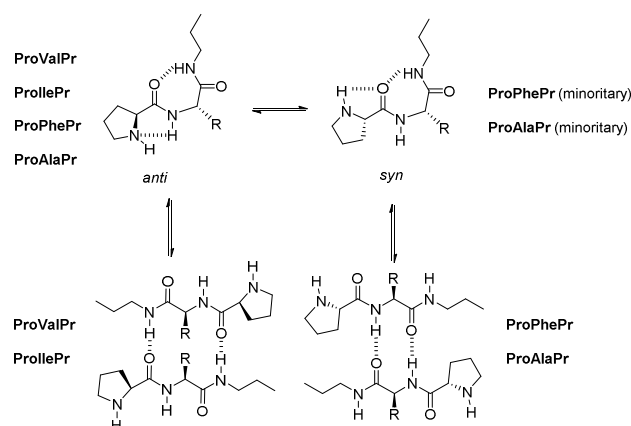


Figure 3. Species distribution diagram for the aggregation of **ProIlePr** in toluene.



Scheme 1. Conformational and aggregation equilibria for the studied peptides.

Similar conformations can be obtained with semiempirical AM1 calculations (not shown). The main difference among the

found conformations is the dihedral angle N-C-C=O of the proline unit, giving place to *syn* and *anti* conformations which present respectively dihedral angles below and above 90°. Additionally *anti* conformation presents an intramolecular hydrogen bond between L-proline amine and the NH of the peptidic linkage as described previously (see Scheme 1).^{12, 14} The existence of this strong intramolecular hydrogen bond can be demonstrated by comparison of the NMR spectra recorded in different solvents. As shown in Figure 4, in difference with NH-a signal, chemical shift of NH-b, which is adjacent to proline ring, is insensitive to solvent polarity, indicating its involvement in intramolecular H-bonding. In this way its interaction with solvent molecules is precluded.

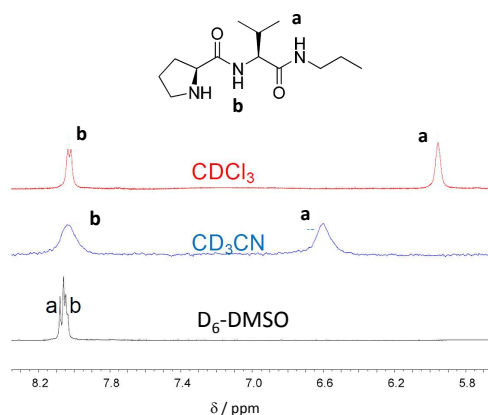


Figure 4. Partial ^1H NMR spectra of **ProValPr** (1 mM) in solvents of different polarity.

On the other hand, *syn* conformation presents an intramolecular hydrogen bond between L-proline amine and the carbonyl CO unit of the peptide linkage.

Structural studies using NMR were carried out to evaluate the presence of these conformations in solution. A whole set of evidences were collected which pointed to the majoritarian presence of folded *anti* conformations in diluted solutions. Firstly, for all the compounds, VT-NMR experiments ($c = 1$ mM, almost no aggregation) revealed a significant variation of both amide signals with temperature indicating their participation in intramolecular H-bonding (see data for **ProllePr** in Figure 5). This fact fits with the presence of *anti* conformations which have two intramolecular H-bonds formed by amide NHs, as depicted in Scheme 1.

Secondly, as shown in the Figure 6, the splitting of the resonances of geminal protons in position 3 of the proline ring also might point to the presence of *anti* disposition. This type of conformation provokes the spatial proximity of C3 protons to the carbonyl, experiencing to a different degree its shielding/deshielding effect. Although this splitting is common in L-proline rings, its magnitude seems to be related to the particular conformation present, as shown below.

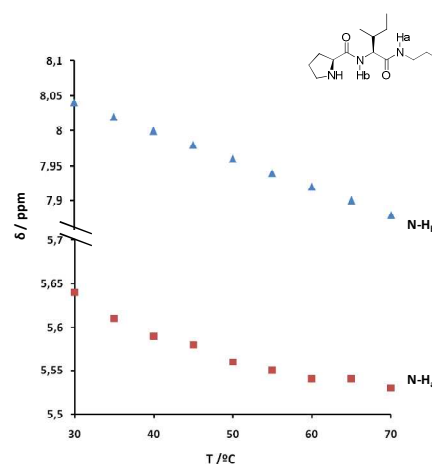


Figure 5. Amide signals shift variation with the temperature of 1 mM **ProllePr** derivative in D_8 -toluene.

Finally, NOE detected between the NH of the propylamide chain and the proton of the chiral carbon of proline (Scheme 1 and Supporting Information, Figure S5) also fits with *anti* conformations which present a shorter distance between these protons in the models (3.8 and 4.5 Å for *anti* and *syn* dispositions respectively). It has to be noted that although NMR data indicate that **ProValPr** and **ProllePr** present almost exclusively *anti* conformation, **ProAlaPr** and **ProPhePr** derivatives present a detectable amount of molecules in *syn* conformation. As seen in Figure 6, peptidic NH signals of **ProAlaPr** and **ProPhePr** present significantly lower chemical shift values than **ProValPr** and **ProllePr** (7.85, 7.92, 8.04 and 8.02 ppm respectively).

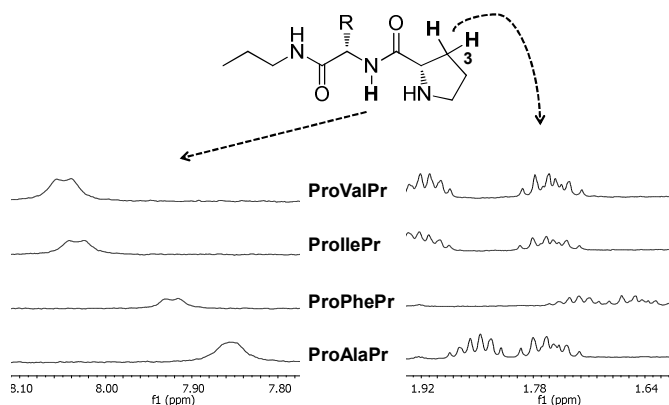


Figure 6. Chemical shift of the amide (left) and the protons at position 3 of the L-proline ring (right) for the different studied compounds (1 mM, D_8 -toluene, 30 °C).

These data point to the weakening of the intramolecular H-bond between the nitrogen atom of proline and the hydrogen atom of the peptide bond that results from *syn* type conformation. Furthermore, the geminal protons at C3 position of the proline ring in **ProAlaPr** and **ProPhePr**, although splitted, present a

reduced difference in chemical shift when compared to **ProValPr** and **ProIlePr** (ca. 0.07 ppm for the former peptides and ca. 0.15 ppm for the latter compounds) pointing again to the coexistence of fast exchanging *syn* and *anti* conformations for the alanine and phenylalanine derivatives (see Scheme 1). The higher steric demand of **Val** and **Ile** side chains (secondary carbon atom attached to chiral centre), compared to **Ala** and **Phe** (methyl and primary carbon atom attached to the chiral centre respectively) can explain the observed differences. In the case of *anti* conformations steric interactions between **Val** or **Ile** side chains and the L-proline ring would arise as indicated by molecular models. (see Supporting Information, Figure S10, for schematic Newman projection).

Analysis of the aggregates by NMR was carried out at a concentration of 70 mM (ca. 80 % of aggregated species). It was found that in all the cases NOE correlations were obtained between protons of propyl chain moiety and protons of proline ring, pointing to the formation of antiparallel aggregates (see Scheme 1 and Supporting Information, Figure S6 and S7). Interestingly, ¹H-NMR spectra of the aggregates formed by **ProPhePr** and **ProAlaPr** show a reduction of the splitting observed for the geminal protons at C3 in the proline ring when compared to spectra from diluted samples (Figure 7). However, for **ProValPr** and **ProIlePr** derivatives the mentioned splitting is maintained upon aggregation. This behaviour points to a conformational change around the L-proline moiety upon aggregation of **ProPhePr** and **ProAlaPr** which might be associated to a transition from *anti* to *syn* type conformations upon aggregation as suggested in Scheme 1.

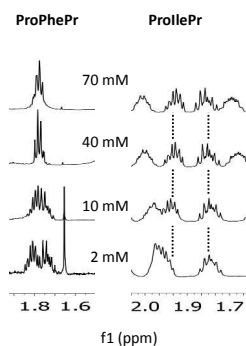


Figure 7. Partial ¹H NMR spectra of **ProPhePr** and **ProIlePr** in D₈-toluene at different concentrations.

Molecular mechanics calculations (AMBER* force field) permit to obtain energy minimized models for the dipeptide dimers studied. In these simulations several intermolecular H-bonds were found. In addition, the spatial proximity of the propyl and proline moieties in the model agrees with NMR NOE experiments. As an example, the structures obtained for **ProIlePr** and **ProAlaPr** are shown in Figure 8.

In order to assess how the conformational preferences and aggregation behaviour affect the catalytic activity of the four dipeptides, the conjugate addition of cyclohexanone to *trans*-β-nitrostyrene was studied in toluene.

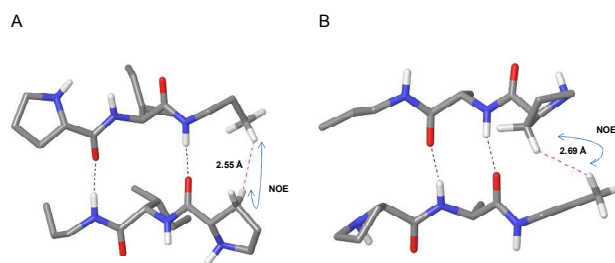
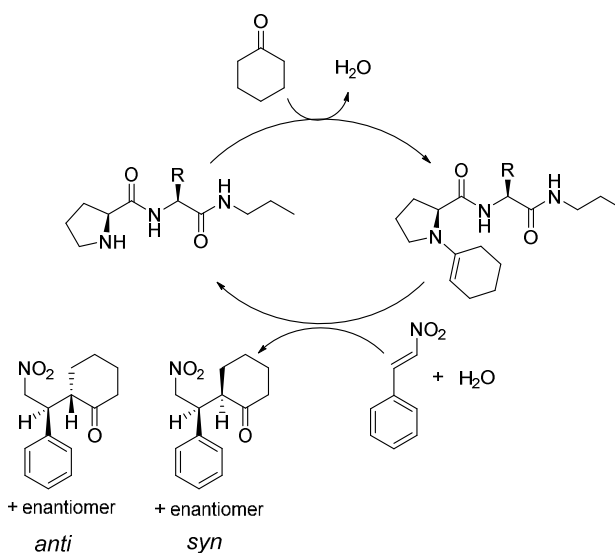


Figure 8. Molecular models for the dimers formed by **ProIlePr** (A) and **ProAlaPr** (B) obtained from molecular mechanics calculations. Non polar hydrogen atoms have been omitted by means of clarity except those involved in NOE contacts.

This reaction has been shown to be catalysed by proline moieties which forms an enamine-type intermediate by reaction with cyclohexanone (Scheme 2).¹³ We reported previously that dipeptide structures provide improvement of catalyst performance when compared with the simple analogue N-propyl-L-prolinamide.¹² For this work it was hypothesized that the different steric demand of the amino acid side chains could influence on the catalytic behaviour by means of different conformational preferences as those discussed above.

In the current work, the *syn* diastereoisomer of the conjugated addition product was very majoritarian in all the cases (see Scheme 2). To evaluate the effect of catalyst aggregation, reaction rates were studied at catalyst concentrations of 1 mM and 5 mM. The studied systems contain in the former case mostly free, non-aggregated catalyst and, in the latter case, a significant amount of aggregated species (ca. 25 %, see Table 1).



Scheme 2. Catalytic cycle for the conjugated addition of cyclohexanone to *trans*-β-nitrostyrene.

The reactions were carried out in the presence of an excess of cyclohexanone and therefore by means of simplicity the system was analysed in terms of pseudo first order kinetics (see equations 1-3; in equation (3) [alkene]_f = concentration at the end of the reaction time, [alkene]₀ = initial concentration, k' = k

[ketone][catalyst]). Indeed the reaction catalysed by **ProIlePr** was monitored *in situ* at regular time intervals by NMR for ca. 60 h and the data fitted well to a first order kinetic model (see Supporting Information, Figure S2). Using the reaction yields under different conditions of catalyst concentration and reaction time the values shown in Figure 9 were obtained.

$$-\frac{d[\text{alkene}]}{dt} = k[\text{catalyst}][\text{ketone}][\text{alkene}] \quad (1);$$

$$-\frac{d[\text{alkene}]}{dt} = k'[\text{alkene}] \quad (2); \text{ (pseudo first order kinetics)}$$

$$\ln \frac{[\text{alkene}]_f}{[\text{alkene}]_0} = -k't \quad (3); \text{ (integrated rate equation)}$$

Noticeable it was observed that upon increasing catalyst concentration from 1 to 5 mM, the kinetic constant of the reaction increased significantly for all the cases, being the catalyst almost inactive for diluted solutions. For example, a 15 fold and 10 fold increase are observed respectively for **ProValPr** and **ProPhePr** when the catalyst concentration grows from 1 to 5 mM. These results point to catalyst activation upon increasing concentration and agree with the fact that aggregates as those shown in Scheme 1 are much more active than non-aggregated species. A rationale for this behaviour is that upon aggregation the catalytic amino centre of proline ring is liberated from the intramolecular H-bonding which prevents its nucleophilic activity (see Scheme 1 and 2).

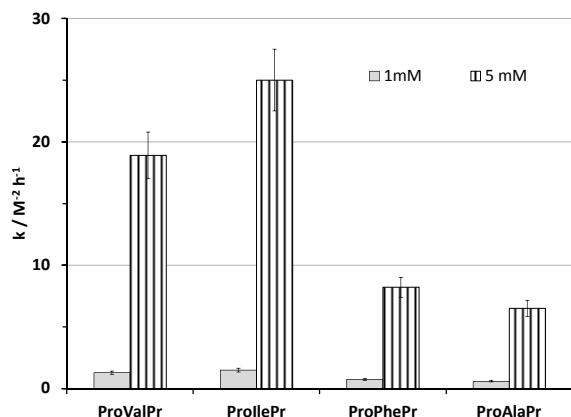


Figure 9. kinetic constants (k , see equation) determined for different concentrations of catalyst in the addition of cyclohexanone to *trans*- β -nitrostyrene at 25 °C in toluene. See details in Experimental Section and Supporting Information.

Additionally, the enantiomeric excess for the reactions carried out with a catalyst concentration of 10 mM are disclosed in Table 2. The reaction showed moderate to poor enantioselectivity but a difference was found for compounds **ProValPr** and **ProIlePr** (*ee* values ca. 30) when compared to **ProPhePr** and **ProAlaPr** derivatives (*ee* values ca. 6). These effects are quite small in terms of transition state energy (ca 0.3-0.4 kcal mol⁻¹) and therefore difficult to rationalize. Perhaps

the hinted conformational differences mentioned above between aggregated **ProPhePr** and **ProAlaPr** (*anti* conformation) when compared to **ProValPr** and **ProIlePr** (*syn* conformation) could be argued to explain in part the changes in selectivity. Enantioselectivity was also measured when the catalysts concentration was varied in the range of 5-30 mM, affording only a slight increase of selectivity upon increasing concentration (see Supporting Information).

Table 2. Enantioselectivity obtained in the addition of cyclohexanone to *trans*- β -nitrostyrene at 25 °C in toluene.^a

Catalyst	Enantiomeric excess ^b
ProValPr	30
ProIlePr	29
ProPhePr	8
ProAlaPr	4

[a] [Cyclohexanone] = 110 mM, [trans- β -nitrostyrene] = 55 mM, [catalyst] = 10 mM. Reaction time 72 h. [b] *syn* (2R, 1'S) enantiomer was majoritary in all the cases.

Conclusions

The structural studies carried out agree well with the experimentally observed catalytic activity of the different dipeptides. In first place, the catalyst activation observed upon increasing the concentration is clearly associated to the aggregation through hydrogen bonding. This process presumably activates the L-proline moiety as a result of the conformational changes associated to the aggregation. NMR studies point to the majoritarian presence of the so called *anti* conformations both for diluted and concentrated solutions of **ProValPr** and **ProIlePr**. In the case of **ProPhePr** and **ProAlaPr** a conformational change from *anti* to *syn* type conformation might be operating upon aggregation. Overall, the results support that organocatalysis can be rather sensitive to concentration and conformational effects associated to minor changes in the catalyst structure. Structurally simple compounds such as the reported dipeptides present a broad scope of species in solution arising both from aggregation and intrinsic conformational mobility.

Experimental Section

General Considerations.

NMR spectra were recorded at 500 MHz, 300 MHz (¹H NMR) and 125 MHz, 75 MHz (¹³C NMR) in different solvents at 30°C with the solvent signals as internal reference. Mass spectra were run in the electrospray (ESMS) mode.

Synthesis.

The catalysts were prepared with conventional peptide chemistry methodology. See Supporting Information for synthetic scheme.

The compound **ProValPr** was synthesized as reported previously.¹⁵

General procedure for the preparation of N-hydroxysuccinimide esters of amino acids. Synthesis of

ZPheOSu: *N*-Cbz-L-phenylalanine (5.21 g, 16.4 mmol) and *N*-hydroxysuccinimide (1.97 g, 16.9 mmol) were dissolved in dry THF (50 mL) at 0°C. Once a clear solution had been obtained, *N,N*-dicyclohexylcarbodiimide (DCC) (3.62 g, 17.3 mmol) in anhydrous THF (10 mL) was added in several aliquots and the resulting solution was stirred at 0–5°C for 3 h. The dicyclohexylurea formed was filtered off and the filtrate was concentrated to dryness. The crude product was recrystallized from 2-propanol to furnish the pure product crystals. (Yield 93%). ZPheOSu compound was previously described in literature and both ¹H and ¹³C NMR spectra were in good agreement with the literature spectra.¹⁶

Synthesis of ZIleOSu: A similar procedure to that described for ZPheOSu was used. Pure crystals were obtained (Yield 89%). ¹H NMR (500 MHz, DMSO-*d*₆) δ 8.04 (d, *J* = 8.2 Hz, 1H), 7.48–7.27 (m, 5H), 5.07 (s, 2H), 4.43–4.30 (m, 1H), 2.81 (s, 4H), 2.04–1.78 (m, 1H), 1.52 (ddd, *J* = 14.5, 9.4, 5.8 Hz, 1H), 1.30 (qd, *J* = 15.3, 7.4 Hz, 1H), 1.01 (dd, *J* = 25.8, 3.8 Hz, 3H), 0.86 (t, *J* = 7.4 Hz, 3H); ¹³C NMR (75 MHz, DMSO-*d*₆) δ 170.3, 168.2, 156.5, 137.1, 128.8, 128.3, 128.2, 66.2, 57.5, 36.8, 25.9, 24.9, 15.3, 11.4; (ESI-TOF, positive mode) *m/z* exp [M + Na]⁺ calcd for C₁₈H₂₂N₂NaO₆⁺ 385.1370; found, 385.1381 [M + Na]⁺, (Δ = 1.3 ppm).

General procedure for the preparation of *N,N'*-Bis(*N*-Cbz-L-aminoacyl) amines. Synthesis of ZPhePr: The *N*-hydroxysuccinimide ester, ZPheOSu, (6.09 g, 15.3 mmol) was dissolved in DME (100 mL). The propylamine (1.0 g, 16.9 mmol) dissolved in DME (20 mL) was added dropwise and the resulting solution was stirred at room temperature for 18 hours and then was warmed for 2 hours at 40–50°C. The solvent was evaporated under vacuum. The resulting solid was dissolved in dichloromethane (25 mL) and washed three times with HCl 0.1 M (3 x 25 mL) and water (3 x 25 mL). The organic phase was dried with magnesium sulfate anhydrous and the solvent was evaporated under vacuum. A white solid was obtained (Yield 93%). ¹H NMR (500 MHz, DMSO-*d*₆) δ 7.92 (t, *J* = 5.5 Hz, 1H), 7.45 (d, *J* = 15.6 Hz, 1H), 7.38–7.10 (m, 10H), 4.99–4.89 (s, 2H), 4.21 (m, 1H), 3.10–2.86 (m, 3H), 2.77 (dd, *J* = 13.6, 10.1 Hz, 1H), 1.45–1.30 (m, 2H), 0.80 (t, *J* = 7.4 Hz, 3H). ¹³C NMR (126 MHz, DMSO-*d*₆) δ 171.5, 156.2, 138.5, 137.5, 129.6, 128.7, 128.4, 128.0, 127.8, 126.6, 65.6, 56.7, 40.7, 38.2, 22.7, 11.7. (ESI-TOF, positive mode) *m/z* exp [M + H]⁺ calcd for C₂₀H₂₅N₂O₃⁺ 341.1865; found, 341.1860 [M + H]⁺, (Δ = 1.5 ppm).

Synthesis of ZIlePr: A similar procedure to that described for ZPhePr was used starting from the *N*-hydroxysuccinimide ester of *N*-Cbz-isoleucine (ZIleOSu). A white solid was obtained (Yield 84%). ¹H NMR (300 MHz, DMSO-*d*₆) δ 7.85 (s, 1H), 7.32 (m, 5H), 7.18 (d, *J* = 8.4 Hz, 1H), 5.01 (s, 2H), 3.80 (t, *J* = 8.1 Hz, 1H), 3.11–2.86 (m, 2H), 1.66 (s, 1H), 1.38 (dd, *J* = 14.3, 7.4 Hz, 3H), 1.03 (m, 1H), 0.95–0.66 (m, 9H); ¹³C NMR (126 MHz, DMSO-*d*₆) δ 171.4, 156.4, 137.5, 128.7, 128.1, 128.0, 65.7, 59.7, 40.6, 36.7, 24.8, 22.6, 15.8, 11.8, 11.3; (ESI-TOF, positive mode) *m/z* exp [M + Na]⁺ calcd for C₁₇H₂₆N₂NaO₃⁺ 329.1836; found, 329.1840 [M + Na]⁺, (Δ = 0.3 ppm).

General procedure to the synthesis of ZAlaPr: To an ice-cooled solution of the corresponding *N*-Cbz-L-alanine (5.03 g, 22.5 mmol) and triethylamine (3.65 mL, 26.3 mmol) in THF (40 mL), a solution of ethyl chloroformate (2.05 mL, 25.7 mmol) in THF (10 mL) was added dropwise with vigorous stirring, a white precipitate was observed. After 30 min stirring in an ice-cold bath, a solution of propylamine (2.15 mL, 26.1 mmol) in THF (10 mL) was added. The mixture was stirred at 0°C for 1 h and was left overnight at room temperature. The resulting white solid solution was filtered and the solvent was evaporated under vacuum. The resulting viscous solid was dissolved in dichloromethane (20 mL) and washed with HCl 0.1 M (3 x 20 mL), KOH 0.1 M (3 x 20 mL), NaHCO₃ (1 x 20 mL) and water (1 x 20 mL). The organic phase was dried with magnesium sulfate anhydrous and the solvent was evaporated under vacuum. The solid obtained was purified by column chromatography (silica gel, hexane/ethyl acetate; 1:1). A white solid compound was obtained. (Yield 35%). ¹H NMR (300 MHz, DMSO-*d*₆) δ 7.76 (s, 1H), 7.45–7.15 (m, 5H), 7.15 (m, 1H), 4.99 (s, 2H), 3.98 (p, *J* = 7.1 Hz, 1H), 3.11–2.85 (m, 2H), 1.50–1.30 (m, 2H), 1.18 (d, *J* = 7.1 Hz, 3H), 0.81 (t, *J* = 7.4 Hz, 3H); ¹³C NMR (75 MHz, DMSO-*d*₆) δ 172.6, 156.0, 137.5, 128.7, 128.1, 65.7, 50.5, 40.6, 22.7, 18.8, 11.7; (ESI-TOF, positive mode) *m/z* exp [M + Na]⁺ calcd for C₁₄H₂₀N₂O₃Na⁺ 287.1366; found, 287.1372 [M + Na]⁺, (Δ = 0 ppm).

General procedure for the deprotection of *N*-Cbz groups. Synthesis of AlaPr: The corresponding *N*-benzyloxycarbonyl protected peptide derivative (0.48 g, 2.15 mmol) and catalytic amount of Pd over activated carbon (5–10% w/w) were placed in a two necked round bottom flask and suspended in MeOH (50 mL). The system was purged to remove the air with N₂ and connected to H₂ atmosphere. The pasty grey suspension was stirred for several hours until it turned completely black (also checked with TLC, MeOH: CH₂Cl₂ (1:4) and revealed with ninhydrin). The black suspension was filtered over Celite and the solvent was evaporated under reduced pressure. The resulting oil was dried in vacuum pump for 24 hours. (Yield 86%). ¹H NMR (300 MHz, DMSO-*d*₆) δ 7.72 (s, 1H), 3.20 (dd, *J* = 13.7, 6.9 Hz, 1H), 3.00 (dd, *J* = 13.6, 6.5 Hz, 2H), 1.52–1.27 (m, 2H), 1.09 (d, *J* = 6.9 Hz, 3H), 0.82 (t, *J* = 7.4 Hz, 3H); ¹³C NMR (75 MHz, DMSO-*d*₆) δ 176.0, 50.7, 40.4, 22.8, 22.1, 11.7; (ESI-TOF, positive mode) *m/z* exp [M + H]⁺ calcd for C₆H₁₅N₂O⁺ 131.1179; found, 131.1181 [M + H]⁺, (Δ = 2.3 ppm).

Synthesis of PhePr: A similar procedure to that described for AlaPr was used. A yellow oil was obtained (Yield 96%). ¹H NMR (300 MHz, DMSO-*d*₆) δ 7.74 (s, 1H), 7.41–6.98 (m, 10H), 3.39 (m, 1H), 3.11–2.80 (m, 3H), 2.60 (dd, *J* = 13.3, 8.0 Hz, 1H), 1.61 (s, 1H), 1.34 (h, *J* = 7.2 Hz, 2H), 0.77 (t, *J* = 7.4 Hz, 3H); ¹³C NMR (126 MHz, DMSO-*d*₆) δ 174.5, 139.2, 129.7, 128.4, 126.4, 56.7, 41.7, 40.5, 22.7, 11.7; (ESI-TOF, positive mode) *m/z* exp [M + H]⁺ calcd for C₁₂H₁₉N₂O⁺ 207.2915; found, 207.1498 [M + H]⁺, (Δ = 0.5 ppm).

Synthesis of IlePr: A similar procedure to that described for AlaPr was used. An oil was obtained (Yield 95%). ¹H NMR (300 MHz, DMSO-*d*₆) δ 7.74 (s, 1H), 3.14–2.87 (m, 3H), 1.57

(dd, $J = 8.9, 3.6$ Hz, 1H), 1.45 – 1.28 (m, 3H), 1.15 – 0.91 (m, 1H), 0.88 – 0.69 (m, 9H); ^{13}C NMR (75 MHz, DMSO- d_6) δ 174.9, 59.8, 40.5, 38.9, 24.2, 22.8, 16.2, 11.9, 11.8; (ESI-TOF, positive mode) m/z exp $[\text{M} + \text{H}]^+$ calcd for $\text{C}_9\text{H}_{21}\text{N}_2\text{O}^+$ 173.1648; found, 176.1656 $[\text{M} + \text{H}]^+$, ($\Delta = 1.2$ ppm).

General procedure for the preparation of N-Boc-protected compounds. Synthesis of BocProAlaPr: A solution of amino amide AlaPr (0.64 g, 4.8 mmol) in dry DME (10 mL) was added dropwise over a solution of Boc-L-Pro-OSu (1.87 g, 5.8 mmol) in dry DME (100 mL). The mixture was stirred at room temperature for 24 h and then at 40 °C for 5 h. The solvent was evaporated under vacuum and the resulting white solid was dissolved in dichloromethane (50 mL) and washed with NaHCO_3 (3 x 15 mL). Afterwards, the organic layers were dried (Na_2SO_4) and the solvent was evaporated under vacuum to yield a white solid product. (Yield 60%). ^1H NMR (300 MHz, DMSO- d_6) δ 7.87 (s, 1H), 7.70 (d, $J = 50.9$ Hz, 1H), 4.55 (dd, $J = 8.9, 3.7$ Hz, 1H), 4.08 (dd, $J = 8.2, 3.4$ Hz, 1H), 3.34 (dd, $J = 14.3, 7.4$ Hz, 2H), 3.00 (dd, $J = 12.8, 6.8$ Hz, 2H), 2.38 (dd, $J = 14.7, 7.3$ Hz, 1H), 2.15 – 1.94 (m, 1H), 1.93 – 1.59 (m, 2H), 1.50 – 1.32 (m, 9H), 1.30 (s, 2H), 1.17 (d, $J = 7.0$ Hz, 3H), 0.80 (t, $J = 7.4$ Hz, 3H); ^{13}C NMR (75 MHz, DMSO- d_6) δ 172.3, 153.7, 78.8, 59.7, 48.4, 46.9, 40.6, 31.3, 28.4, 25.7, 22.7, 19.1, 11.68, 11.7; (ESI-TOF, positive mode) m/z exp $[\text{M} + \text{H}]^+$ calcd for $\text{C}_{16}\text{H}_{30}\text{N}_3\text{O}_4^+$ 328.2231; found, 328.2237 $[\text{M} + \text{H}]^+$, ($\Delta = 0.3$ ppm).

Synthesis of BocProPhePr: A similar procedure to that described for BocProAlaPr was used. A white solid product was obtained (Yield 95%). ^1H NMR (300 MHz, DMSO- d_6) δ 7.88 (s, 1H), 7.80 (d, $J = 8.2$ Hz, 1H), 7.22 (q, $J = 8.7$ Hz, 5H), 4.01 (dd, $J = 8.7, 3.3$ Hz, 1H), 3.41 (m, 1H), 3.24 – 2.89 (m, 6H), 2.00 (s, 1H), 1.64 (d, $J = 12.8$ Hz, 3H), 1.36 (dd, $J = 14.1, 5.9$ Hz, 6H), 1.22 (d, $J = 11.9$ Hz, 5H), 0.76 (t, $J = 7.4$ Hz, 3H); ^{13}C NMR (75 MHz, DMSO- d_6) δ 172.4, 171.1, 153.8, 138.2, 129.5, 128.4, 126.6, 78.8, 60.1, 54.3, 46.9, 38.4, 31.2, 28.3, 23.3, 22.6, 11.7; (ESI-TOF, positive mode) m/z exp $[\text{M} + \text{Na}]^+$ calcd for $\text{C}_{22}\text{H}_{33}\text{N}_3\text{O}_4\text{Na}^+$ 426.2363; found, 426.2365 $[\text{M} + \text{Na}]^+$, ($\Delta = 0.9$ ppm).

Synthesis of BocProPhePr: A similar procedure to that described for BocProAlaPr was used. A white solid product was obtained (Yield 89%). ^1H NMR (500 MHz, DMSO- d_6) δ 8.02 – 7.79 (m, 1H), 7.61 (d, $J = 20.3$ Hz, 1H), 4.29 – 3.98 (m, 1H), 3.51 – 3.30 (m, 1H), 3.09 – 2.87 (m, 2H), 2.76 (d, $J = 27.1$ Hz, 2H), 2.16 – 1.95 (m, 1H), 2.01 – 1.57 (m, 4H), 1.48 – 1.20 (m, 12H), 1.17 – 1.00 (m, 1H), 0.93 – 0.68 (m, 9H); ^{13}C NMR (126 MHz, DMSO- d_6) δ 172.4, 171.1, 153.8, 80.2, 59.9, 57.2, 46.9, 40.6, 37.1, 31.5, 28.1, 25.9, 24.9, 22.6, 15.8, 11.7, 11.2; (ESI-TOF, positive mode) m/z exp $[\text{M} + \text{Na}]^+$ calcd for $\text{C}_{19}\text{H}_{35}\text{N}_3\text{O}_4\text{Na}^+$ 392.2520; found, 392.2527 $[\text{M} + \text{Na}]^+$, ($\Delta = 0.5$ ppm).

General procedure for the deprotection of N-Boc groups.

Synthesis of ProAlaPr: N-protected compound BocProAlaPr (2.00 g, 7.8 mmol) was dissolved in dichloromethane (50 mL) and after addition of TFA (15 mL) the mixture was stirred at room temperature for 2 h. The solvent was evaporated under vacuum and then the resulting crude oil

was dissolved in water (50 mL). The solution was treated with NaOH (pH = 12), and extracted with chloroform (3 x 15 mL). The organic layers were washed with water and dried (Na_2SO_4). The solvent was evaporated under vacuum to yield a white solid compound. (Yield 66%). ^1H NMR (500 MHz, DMSO- d_6) δ 8.09 (d, $J = 7.7$ Hz, 1H), 7.84 (d, $J = 97.2$ Hz, 1H), 4.37 – 4.14 (m, 1H), 3.60 – 3.38 (m, 1H), 3.09 – 2.96 (m, 2H), 2.90 – 2.80 (m, 1H), 2.77 – 2.67 (m, 1H), 2.06 – 1.85 (m, 1H), 1.70 – 1.60 (m, 1H), 1.61 – 1.52 (m, 2H), 1.46 – 1.31 (m, 2H), 1.28 – 1.04 (m, 3H), 0.83 (td, $J = 7.4, 2.1$ Hz, 3H); ^{13}C NMR (75 MHz, DMSO- d_6) δ 174.4, 172.5, 61.0, 48.3, 47.3, 41.3, 30.9, 26.2, 22.8, 19.8, 11.8; (ESI-TOF, positive mode) m/z exp $[\text{M} + \text{H}]^+$ calcd for $\text{C}_{11}\text{H}_{22}\text{N}_3\text{O}_2^+$ 228.1707; found, 228.1712 $[\text{M} + \text{H}]^+$, ($\Delta = 0.9$ ppm).

Synthesis of ProPhePr: A similar procedure to that described for ProAlaPr was used. A white solid product was obtained (Yield 68%). ^1H NMR (300 MHz, DMSO- d_6) δ 8.00 (dd, $J = 14.5, 7.4$ Hz, 2H), 7.30 – 7.02 (m, 5H), 4.48 (td, $J = 8.6, 5.5$ Hz, 1H), 3.43 (dt, $J = 23.6, 11.7$ Hz, 1H), 3.12 – 2.86 (m, 3H), 2.85 – 2.69 (m, 3H), 2.65 – 2.53 (m, 1H), 1.81 (tt, $J = 7.9, 7.5$ Hz, 1H), 1.52 – 1.20 (m, 5H), 0.79 (t, $J = 7.4$ Hz, 3H); ^{13}C NMR (126 MHz, DMSO- d_6) δ 174.1, 170.9, 137.7, 129.6, 128.3, 126.7, 60.4, 53.2, 46.9, 40.7, 38.9, 30.6, 26.0, 22.6, 11.7; (ESI-TOF, positive mode) m/z exp $[\text{M} + \text{H}]^+$ calcd for $\text{C}_{17}\text{H}_{26}\text{N}_3\text{O}^+$ 304.2020; found, 304.2027 $[\text{M} + \text{H}]^+$, ($\Delta = 0.7$ ppm).

Synthesis of ProllePr: A similar procedure to that described for ProAlaPr was used. A white solid product was obtained (Yield 52%). ^1H NMR (500 MHz, DMSO- d_6) δ 8.13 – 7.89 (m, 2H), 4.11 (ddd, $J = 25.7, 13.2, 7.8$ Hz, 1H), 3.53 (dd, $J = 9.0, 5.0$ Hz, 1H), 3.14 – 2.91 (m, 2H), 2.91 – 2.84 (m, 1H), 2.72 (dt, $J = 10.2, 6.4$ Hz, 1H), 1.94 (ddd, $J = 16.3, 12.4, 7.5$ Hz, 1H), 1.78 – 1.64 (m, 2H), 1.63 – 1.48 (m, 2H), 1.48 – 1.28 (m, 3H), 1.08 – 0.91 (m, 1H), 0.81 (dq, $J = 11.8, 7.3$ Hz, 9H); ^{13}C NMR (300 MHz, DMSO) δ 174.2, 171.0, 60.6, 56.2, 47.1, 40.5, 37.8, 31.0, 26.3, 24.6, 22.6, 15.8, 11.8, 11.3; (ESI-TOF, positive mode) m/z exp $[\text{M} + \text{H}]^+$ calcd for $\text{C}_{14}\text{H}_{28}\text{N}_3\text{O}^+$ 270.2176; found, 270.2186 $[\text{M} + \text{H}]^+$, ($\Delta = 1.5$ ppm).

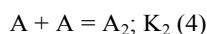
General procedure for the 1,4-conjugated Michael addition reaction.¹² Catalyst (0.033 mmol) was dissolved in a vial using the amount of toluene required to reach the targeted final concentration (for diluted systems, 1 mM and 2.5 mM, 0.006 mmol of catalyst were added). Then, *trans*- β -nitrostyrene (0.16 mmol) and cyclohexanone (3.29 mmol) were added and the reaction was left at room temperature the required time. The reaction was quenched by addition of a 0.25 M aqueous acetic acid solution (2 mL) and toluene (1 mL). The aqueous layer was extracted with toluene (2 x 2 mL). Then the solvent of the combined organic extracts were removed until dryness. The reaction crude was analyzed by ^1H -NMR in CDCl_3 in order to determine the yield and the diastereoselectivity (*syn* = 3.76 ppm; *anti* = 4.01 ppm)¹⁷ and was further purified by column chromatography (silica gel, mixture of hexane/ethyl acetate, 3:1) to isolate the pure product used to determine enantioselectivity.

Determination of the enantiomeric excess.¹² The enantiomeric excess was determined by HPLC using a Chiral Pack IA column, hexane/IPA (v/v: 85/15), flow rate= 1 mL/min, λ = 210 nm, t_1 = 7.76 min (2S, 1'R), t_2 = 8.76 min (2R, 1'S).

Kinetic studies. Kinetic constants were estimated from the reaction yield at a given final time. The concentration of cyclohexanone was approximated to be constant and the system analyzed as having a pseudo first order kinetics.

NMR studies ^1H and ^{13}C NMR spectra were recorded in a Varian Mercury 300 MHz or Varian Inova 500 MHz spectrometer at 30 °C. NOESY-1D experiments were recorded using a mixing time of 800 ms at 30 °C.

Determination of aggregation constants. The NMR chemical shift of the NH signal from the propylamide unit in D₈-toluenewas used as a probe for the determination of the association constants. The samples were prepared dissolving the required amount of catalyst in toluene and were left overnight at r.t. A set of data corresponding to at least 10 different concentrations were acquired at 30 °C. The results could be fitted to a cooperative binding model using the equations reported previously in the literature¹⁸ (see Supporting Information). The equations were solved by non-linear regression with Solver (Microsoft Excel) to afford K_2 (dimerization constant, see equation (4)), K_n (successive oligomerization constant, see equation (5)) and maximum chemical shift (δ_{max}).



Molecular modeling studies. The models reported were obtained by molecular mechanics calculations performed with MacroModel using AMBER* as force field. Exhaustive Monte Carlo conformational search (1000 steps of torsional angles variation) was carried out for the isolated molecules. The structures described for the folded conformations in scheme 1 and Supporting Information correspond to energy minimized structures near the global minimum (within ca. 10 kJmol⁻¹). The models for the aggregates shown in Figure 8 were built manually from unfolded energy minimized conformers. Then the dimeric structures were energy minimized to the nearest local energy minimum. The feasibility of the molecular mechanics models was checked with AM1 semiempirical energy minimizations which afforded basically similar conformations within a similar energy range.

Acknowledgments

Ministry of Science and Innovation of Spain (grant CTQ2012-37735) and Universitat Jaume I (grants P1.1B2012-25 and P1.1B2013-57) are thanked for financial support. Cristina

Berdugo thanks Ministry of Science and Innovation of Spain for a PhD fellowship (FPI program).

Notes and references

^aDepartament de Química Inorgànica i Orgànica, Universitat Jaume I, Avda. SosBaynat s/n, Castelló, 12071 Spain

Fax: +34964728214

E-mail: miravet@uji.es; escuder@uji.es

Homepage: <http://supra.uji.es>

†Electronic Supplementary Information (ESI) available: See

DOI: 10.1039/b000000x/

- (a) S. Mukherjee, J. W. Yang, S. Hoffmann and B. List, *Chem. Rev.*, 2007, **107**, 5471-5569; (b) W. Notz, F. Tanaka and C. F. Barbas III, *Acc. Chem. Res.*, 2004, **37**, 580-591.
- H. Wennemers, *Chem. Commun.*, 2011, **47**, 12036-12041.
- B. List, P. Pojarliev and H. J. Martin, *Org. Lett.*, 2001, **3**, 2423-2425.
- H. J. Martin and B. List, *Synlett*, 2003, 1901-1902.
- (a) R. Kastl, Y. Arakawa, J. Duschmale, M. Wiesner and H. Wennemers, *Chimia*, 2013, **67**, 279-282; (b) J. Duschmale and H. Wennemers, *Chem. Eur. J.*, 2012, **18**, 1111-1120; (c) M. Wiesner, J. D. Revell and H. Wennemers, *Angew. Chem. Int. Ed.*, 2008, **47**, 1871-1874; (d) M. Wiesner, M. Neuburger and H. Wennemers, *Chem. Eur. J.*, 2009, **15**, 10103-10109.
- (a) S. B. Otvos, I. M. Mandity and F. Fulop, *ChemSusChem*, 2012, **5**, 266-269; (b) Y. Arakawa and H. Wennemers, *ChemSusChem*, 2013, **6**, 242-245.
- F. Bachle, J. Duschmale, C. Ebner, A. Pfaltz and H. Wennemers, *Angew. Chem. Int. Ed.*, 2013, **52**, 12619-12623.
- (a) H. S. Rho, S. H. Oh, J. W. Lee, J. Y. Lee, J. Chin and C. E. Song, *Chem. Commun.*, 2008, 1208-1210; (b) H. B. Jang, H. S. Rho, J. S. Oh, E. H. Nam, S. E. Park, H. Y. Bae and C. E. Song, *Org. Biomol. Chem.*, 2010, **8**, 3918-3922; (c) G. Tarkanyi, P. Kiraly, T. Soos and S. Varga, *Chem. Eur. J.*, 2012, **18**, 1918-1922.
- (a) S. H. Oh, H. S. Rho, J. W. Lee, J. E. Lee, S. H. Youk, J. Chin and C. E. Song, *Angew. Chem. Int. Ed.*, 2008, **47**, 7872-7875; (b) J. S. Oh, J. W. Lee, T. H. Ryu, J. H. Lee and C. E. Song, *Org. Biomol. Chem.*, 2012, **10**, 1052-1055.
- T. Satyanarayana, S. Abraham and H. B. Kagan, *Angew. Chem. Int. Ed.*, 2009, **48**, 456-494.
- E. G. Doyagüez, G. Corrales, L. Garrido, J. Rodríguez-Hernández, A. Gallardo and A. Fernández-Mayoralas, *Macromolecules*, 2011, **44**, 6268-6276.
- F. Rodríguez-Llansola, J. F. Miravet and B. Escuder, *Chem. Eur. J.*, 2010, **16**, 8480-8486.
- (a) M. E. Kuehne and L. Foley, *J. Org. Chem.*, 1965, **30**, 4280-4284; (b) A. P. Carley, S. Dixon and J. D. Kilburn, *Synthesis-Stuttgart*, 2009, 2509-2516; (c) N. Mase, K. Watanabe, H. Yoda, K. Takabe, F. Tanaka and C. F. Barbas III, *J. Am. Chem. Soc.*, 2006, **128**, 4966-4967.
- F. Rodríguez-Llansola, J. F. Miravet and B. Escuder, *Chem. Commun.*, 2009, 209.
- (a) B. Escuder, S. Marti and J. F. Miravet, *Langmuir*, 2005, **21**, 6776-6787; (b) F. Rodríguez-Llansola, B. Escuder and J. F. Miravet, *J. Am. Chem. Soc.*, 2009, **131**, 11478-11484.

- 16 J. Becerril, M. Bolte, M. I. Burguete, F. Galindo, E. García-España, S. V. Luis and J. F. Miravet, *J. Am. Chem. Soc.*, 2003, **125**, 6677-6686.
- 17 A. J. Cobb, D. M. Shaw, D. A. Longbottom, J. B. Gold and S. V. Ley, *Org. Biomol. Chem.*, 2005, **3**, 84-96.
- 18 (a) M. de Loos, J. van Esch, R. M. Kellogg and B. L. Feringa, *Angew. Chem. Int. Ed.*, 2001, **40**, 613-616; (b) M. Akiyama and T. Ohtani, *Spectrochimica Acta Part A: Molecular Spectroscopy*, 1994, **50**, 317-324.